Multi-Walled Carbon Nanotube Coating on Alkali Treated TiO₂ Nanotubes Surface for Improvement of Biocompatibility

Jung-Eun Park [1,2,3,4,†] (ID), **Yong-Seok Jang** [1,2,3,4,†], **Tae-Sung Bae** [1,2,3,4] and **Min-Ho Lee** [1,2,3,4,*]

[1] Department of Dental Biomaterials, School of Dentistry, Chonbuk National University, Jeonju 54896, Korea; pje312@naver.com (J.-E.P.); yjang@jbnu.ac.kr (Y.-S.J.); bts@jbnu.ac.kr (T.-S.B.)

[2] Institute of Biodegradable Material, School of Dentistry, Chonbuk National University, Jeonju 54896, Korea

[3] Institute of Oral Bioscience, School of Dentistry, Chonbuk National University, Jeonju 54896, Korea

[4] BK21 Plus Project, School of Dentistry, Chonbuk National University, Jeonju 54896, Korea

* Correspondence: mh@jbnu.ac.kr; Tel.: +82-632-704-042; Fax: +82-632-704-040

† These authors contributed equally to this work.

check for updates

Abstract: The aim of this study is to enhance the bioactivity of pure titanium using multiple surface treatments for the application of the implant. To form the biofunctional multilayer coating on pure titanium, anodization was conducted to make titanium dioxide nanotubes, then multi-walled carbon nanotubes were coated using a dipping method after an alkali treatment. The surface characteristics at each step were analyzed using a field emission scanning electron microscope and X-ray diffractometer. The effect of the multilayer coating on the biocompatibility was identified using immersion and cytotoxicity tests. Better hydroxyapatite formation was observed on the surface of multilayer-coated pure titanium compared to non-treated pure titanium after immersion in the simulated body fluid. Improvement of biocompatibility by multiple surface treatments was identified through various cytotoxicity tests using osteoblast cells.

Keywords: anodization; TiO₂ nanotubes; alkali treatment; carbon nanotube; biocompatibility

1. Introduction

Material surfaces should have the optimal biocompatibility in vivo with the surrounding biological environment because the implant surface is in direct contact with biological tissue. In addition, the implant surface should allow for the physical, chemical, and electrical properties, as well as the increased biological activities induced by interactions between the material surface and the tissue. Titanium is used as a material possessing these properties and is best suited for applications in the orthopedic and dental fields, it is also widely used as a bone replacement material [1–3]. A thin nanoscale TiO₂ film is formed on the titanium surface upon exposure to air by reacting it with oxygen while it is being made into an implant. However, naturally occurring thin TiO₂ films have a heterogeneous composition and a low density. Therefore, methods for achieving thin TiO₂ films with dense structures of homogeneous compositions have been studied to improve titanium's biocompatibility. Moreover, because of the bio-inert character of natural thin TiO₂ films, it takes months until osseointegration sets in, thus prolonging the duration of the prosthetic treatment by up to several months. A number of studies have been conducted to overcome this problem by inducing bioactive property and enhancing the bone–implant adhesion through the surface modification of titanium implants [4,5]. Because such an implant surface accelerates osseointegration and enhances bone–implant adhesion, various surface-treatment methods have been studied, including surface coating, surface microstructure modification, and chemical property modification [6–8].

Anodization is one of a variety of surface treatment methods; it is an electrochemical method in which the passive films formed by anodization and cathodic reduction reactions enhance the corrosion resistance of the surface. Furthermore, various surfaces can be obtained depending on voltage, current, time, temperature, and electrolyte type. The anodization of titanium forms nanotubes on the surface and increases its roughness and wettability [8]. According to previous study results, anatase TiO_2 nanotubes, which can be obtained by heat-treating anodized TiO_2 nanotubes, increase the contact area with cells and thus promote interaction with osteoblasts [9,10].

In the alkali treatment method, which is a chemical surface treatment method, the titanium surface is soaked in a NaOH solution and the surface property is modified through ionic reaction. Bioactive sodium titanate gel layers with alkali ions are formed on the NaOH-treated titanium surface, and the surface layer composition and structure are modified through densification [11–14]. Na_2TiO_3 formed on the alkali-treated titanium surface increases the surface roughness and improves the contact property. Moreover, Na deposited on the surface forms sites within the body where the substitution of Ca and P ions is induced, thereby promoting the precipitation of hydroxyapatite (HAp) inducing osseointegration. This process can be accelerated by heat treatment [11,15]. However, it was reported that an alkali-treated surface releases Na ions into the body, resulting in a slowing down of cell proliferation [16]. In another study related to Na ion extraction, biocompatibility could be improved by water treatment to accelerate HAp formation [17].

Carbon nanotubes (CNTs) are tubular cylinders of carbon atoms forming hexagonal beehive-like structures, with each hexagon comprising six carbon atoms in which one atom is symmetrically bound to the other three atoms. They are representative new materials discovered by Iijima in 1991 [18], and their extraordinary electrical, mechanical, and thermal properties based on their unique molecular structure have instigated research worldwide. They are promising candidates as new materials for applications in a wide range of industries such as information and communication technology, electronic devices, biosensors, transistors, hydrogen storage batteries, environmental fields, energy, and medicine. Not only do they have superior properties as industrial materials, but they also have unlimited potential as biomaterials. They have a wide spectrum of biological and medical applications. Specifically, CNT-based cell culture, drug delivery systems, implants, and bone formation are rapidly developing areas of research. They are also studied as a scaffold material in regenerative medicine [19,20]. Multi-walled CNT (MWCNT)-coated titanium has been reported to show stronger cell adhesion than untreated titanium [3], and another study [20] experimentally proved the feasibility of CNTs as biomaterials in in vitro and in vivo tests. On the basis of the results of these previous studies, it was hypothesized that a CNT coating on surface-treated titanium improves biocompatibility of the implant.

Therefore, in this study, the surface of pure titanium was modified by anodization, alkali treatment, and Multiwall Carbon Nanotubes (MWCNT) coating to form the biofunctional multilayer for dental and orthopedic applications. The modified surfaces of Ti were characterized by SEM, XRD, and AFM; the biocompatibility of the modified surfaces was evaluated with a cytotoxicity test using osteoblast.

2. Materials and Methods

2.1. Surface Modification

Anodizing treatment: Specimens (dimension: 10 mm × 10 mm × 2 mm) were fabricated with grade II commercially pure titanium (PT), and their surface homogeneity was ensured by polishing them with SiC paper (#400–#1000 grit), followed by an ultrasonic wash with acetone and distilled water and drying. To form nanotubes on the titanium surface, the titanium specimens were connected to a platinum plate used as the anodic metal with a DC power supply (SDP-303D, Daunanotck, Bucheon, Korea). The electrolyte was prepared by adding NH_4F (1 wt %) to 79 wt % glycerol and 20 wt % distilled water. TiO_2 nanotubes (NT) were formed by applying a voltage of 20 V for 1 h.

Alkali treatment: Titanium specimens were soaked in a 5 M NaOH solution in an incubator (60 °C) for 24 h for alkali treatment, followed by a wash with distilled water and drying in the air. The surface-treated titanium specimens were then subjected to a heat treatment at 500 °C for 2 h to enhance binding between the TiO_2 nanotube column and alkali layer [4].

Silane treatment: Treated specimens were placed on a 120 °C hot plate and reacted with 0.25 M 3-aminopropyltriethoxysilane (APTES, Sigma Aldrich, Saint Louis, MO, USA) pH-adjusted at 3.0 with an HCl solution by dropping 150 μL APTES three times on their surface. The residual APTES was rinsed off with distilled water, and the specimens were dried on a 60 °C hot plate. They were then saline-treated to improve the adhesion between the titanium surface and CNTs.

2.2. MWCNTs Preparation

To fabricate the test specimens by introducing the carboxyl functional group (COOH) on the surface of MWCNTs (CNT Co., LTD., Yeonsu-Go, Incheon, Korea), the MWCNTs were subjected to ultrasonic treatment in a round flask containing a 60% nitric acid solution for 30 min and stirred at 120 °C for 8 h afterwards. Then the MWCNTs were rinsed to reach pH 7 and vacuum-dried at 55 °C. The prepared specimens, as described in Section 2.1, were then soaked in ethanol dispersed with MWCNT–COOH for 3 h and coated with MWCNTs. Specimens thus prepared with four different treatments were labeled as, PT (pure titanium group), PTN (TiO_2 NT), PTNA (TiO_2 NT + alkali treatment), PTNAC (TiO_2 NT + alkali treatment + MWCNTs coating group).

2.3. Characterization of Surface

The surface morphology of the surface-treated titanium specimens was observed by a field emission scanning electron microscope (FE-SEM, SU-70, HITACHI, Tykyo, Japan). Crystalline structure was identified using an X-ray diffractometer (XRD, X'pert Powder, PANalytical, Almelo, The Netherlands). The surface roughness of each specimen was measured using a profilometer (SV-528, Mitutoyo, Kawasaki, Japan). The surface structure was examined using atomic force microscopy (AFM; MultiMode + Bioscope, Digital Instruments, Santa Barbara, CA, USA) at the speed of approximately 1 Hz and within a range of $5 \times 5\ \mu m^2$. Wettability and surface energy were observed by contact angle (phoenlx-300, SEO, Gwangju, Korea).

2.4. In Vitro Test

2.4.1. Simulated Body Fluid (SBF) Solution Immersion Test

Bioactivity was tested by soaking each surface-treated titanium specimen in a simulated body fluid (SBF) solution and analyzing the formation on the surface. The SBF solution was prepared by adding 0.285 g/L calcium chloride dehydrate, 0.09767 g/L magnesium sulfate, and 0.350 g/L sodium hydrogen carbonate to Hanks' solution (H2387, Sigma Chemical Co., St. Louis, MO, USA) and the ionic concentration was adjusted to pH 7.4. All specimens were immersed in the SBF solution for 7 and 10 days. After the immersion treatment, the precipitation of bone-like apatite was analyzed using XRD. The film composition was studied with an FE-SEM after coating them with platinum.

2.4.2. Cell Culture

Cytotoxicity was assessed using the mouse osteoblastic cell line MC3T3-E1. As a culture medium, fetal bovine serum (FBS, Gibco Co., Grand Island, NY, USA) with 10% nutrient proportion including penicillin was mixed with α-modified minimum essential medium (α-MEM, Gibco Co., Grand Island, NY, USA). The cell culture was performed in an incubator (3111, Thermo Electron Corporation, Waltham, MA, USA) at 37 °C in a 5% CO_2 environment.

2.4.3. Cell Proliferation Test (WST Assay)

Reactions to the proliferation of cells adhered to the specimens were analyzed with water soluble tetrazolium (WST) assay. Each surface-treated specimen underwent 24-h ultraviolet disinfection, and cells were seeded at the concentration of 5×10^{-4} cell·mL^{-1} per specimen. After removing the culture medium after 2- and 5-day cultures, 500 μL solution mix of WST assay (Premix WST-1, TaKaRa, Shiga, Japan) and α-MEM was dispensed, which was then left to react in 5% CO_2 incubator for 1 h. The absorbance of the reacted medium was measured at 450 nm using an enzyme-linked immunosorbent assay (ELISA) reader (Molecular devices, EMax, San Jose, CA, USA).

2.4.4. Cell Adhesion Test

A cell adhesion test was performed to assess the specimen–cell adhesion in the initial phase. Cells were seeded in the same manner as with the WST assay. After 48 h, the culture medium was removed and the specimens were washed with phosphate-buffered saline (PBS). They were left to react with added 0.02% TryLE™ Express (TE, Gibco Co., Grand Island, NY, USA) for 5 min. A WST assay was then performed on each specimen.

2.4.5. Cell Morphology Observation

In order to observe cell morphologies, cells were seeded in the same manner as for the WST assay, and observations were made after 2- and 5-day cell culture. After removing the medium and flushing off non-adherent cells and suspension three times with PBS, the adherent cells were fixed first in 2.5% glutaraldehyde for 2 h at 4 °C, followed by the second fixation in 1% osmium tetroxide for 1 h at 4 °C. The fixed cells were dehydrated under increasing alcohol concentrations (50%, 60%, 70%, 80%, 90%, 100%) and the adhesion status of the cells could be observed with an FE-SEM.

2.4.6. Statistical Analysis

All experiments were performed in triplicate and statistically analyzed with a one-way ANOVA ($p < 0.05$).

3. Result

The surface morphologies of PT, PTN, PTNA, and PTNAC were observed with FE-SEM as shown Figure 1. A smooth structure was observed on the surface of PT (Figure 1A). An array of homogenous TiO_2 nanotubes was formed on the surface by anodization and the thickness of coating layer was about 600 nm (Figure 1B). A nano-fibrous structure was formed on anodized Ti by alkali treatment in the 5 M NaOH solution, and an oxidized layer and an alkali layer was densely combined (Figure 1C). The surface coated MWCNTs after anodization with Ti and alkali treatment showed a more complex network, more rigid than the PTN group (Figure 1D).

Figure 2 shows the XRD patterns of PT, PTN, PTNA, and PTNAC. Ti peaks were observed in all groups. Rutile and anatase phases were observed on the PTN surface (Figure 2B). An anatase phase and Na_2TiO_3 phase were observed but rutile was not observed in PTNA and PTNAC (Figure 2C,D).
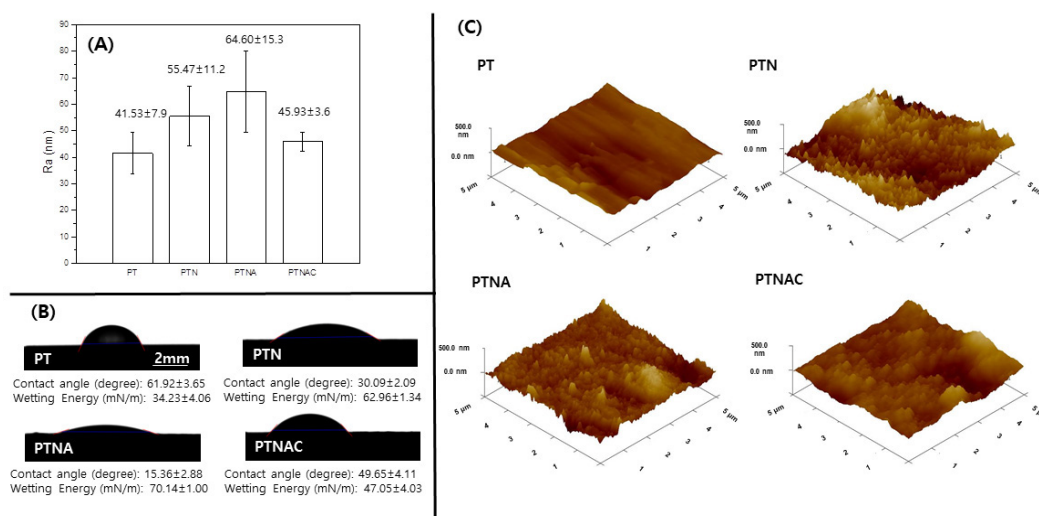
Figure 3 shows the value of the surface roughness, contact angle, and a 3D image of PT, PTN, PTNA, and PTNAC. The surface roughness values of PT, PTN, PTNA, and PTNAC are 41.53 ± 7.9, 55.47 ± 11.2, 64.60 ± 15.3, and 45.93 ± 3.6, respectively. The surface roughness was gradually increased by anodization and alkali treatment, but it was decreased by the MWCNT coating. Contact angle values of PT, PTN, PTNA, and PTNAC are 61.92 ± 3.65, 30.09 ± 2.09, 15.36 ± 2.88, and 49.65 ± 4.11; and the wetting energy values are 34.23 ± 4.06 mN/m, 62.96 ± 1.34 mN/m, 70.14 ± 1.00 mN/m, and 47.05 ± 4.03 mN/m, respectively. The smaller the contact angle of the surface, the higher the wetting energy value.
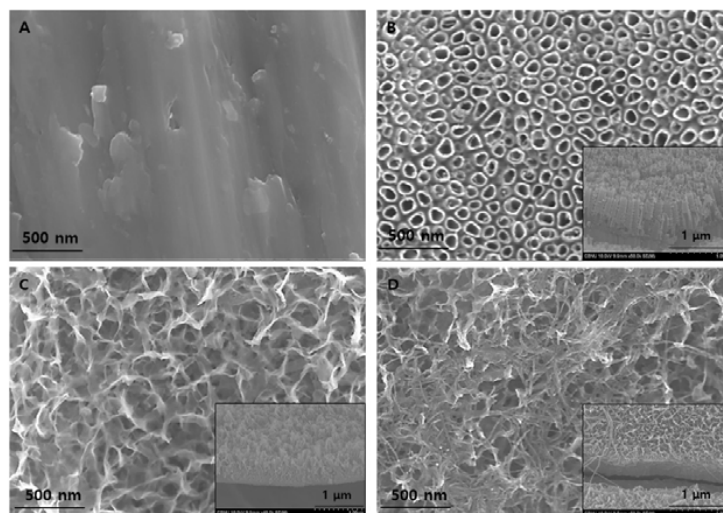
Figure 1. Field emission scanning electron microscope (FE-SEM) images of surfaces of different specimens: (**A**) Pure titanium (PT); (**B**) TiO$_2$ nanotubes (PTN); (**C**) TiO$_2$ nanotubes + alkali treatment (PTNA); and (**D**) TiO$_2$ nanotubes + alkali treatment + multiwall carbon nanotubes coating (PTNAC).
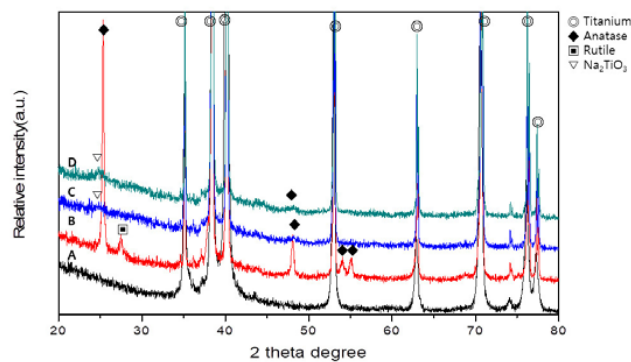

Figure 2. XRD patterns of difference specimens: (A) PT; (B) PTN; (C) PTNA; and (D) PTNAC.

Figure 3. (**A**) Surface roughness value; (**B**) contact angle; (**C**) and atomic force microscopy (AFM) image of PT and surface-treated (PTN, PTNA, and PTNAC) specimens.

Figure 4 shows the FE-SEM images of the surface (A and E) of the PT, (B and F) of the PTN, (C and G) of the PTNA, and (D and H) of the PTNAC after immersion in the SBF solution for 7 and 10 days. A flat structure was observed on the surface of PT, but precipitates were confirmed on the surface of PTN, PTNA, and PTNAC after immersion for 7 days. Precipitates were observed on the surface of PT after immersion for 10 days (Figure 4E), but precipitates on the surface of the other groups were confirmed after immersion for 7 days (Figure 4B–D). Precipitates covered the entire surface of all the groups after immersion for 10 days.
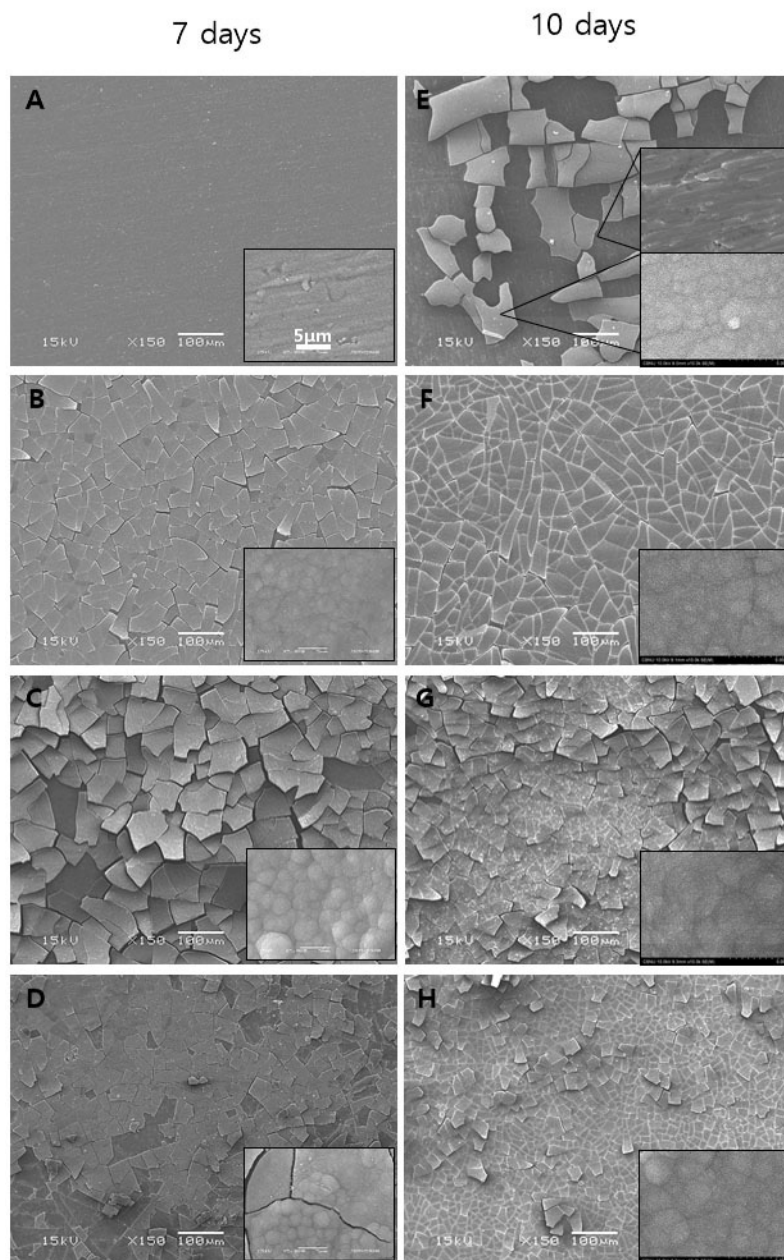
Figure 4. FE-SEM images of (**A**,**E**) PT, (**B**,**F**) PTN, (**C**,**G**) PTNA, and (**D**,**H**) PTNAC specimens surfaces after immersion in simulated body fluid (SBF) for (**A**–**D**) 7 and (**E**–**H**) 10 days.

Figure 5 shows the XRD pattern of the surfaces after immersion in SBF for 7 and 10 days. Peaks related to the hydroxyapatite phase and Tricalcium phosphate (TCP) phase were confirmed on PTN, PTNA, and PTNAC but were not on PT after 7 days. Also, peaks related to the hydroxyapatite

phase and TCP phase were observed on PTN, PTNA, and PTNAC after 10 days. A peak related to the TCP phase were confirmed on PT but a hydroxyapatite phase was not confirmed on PT.
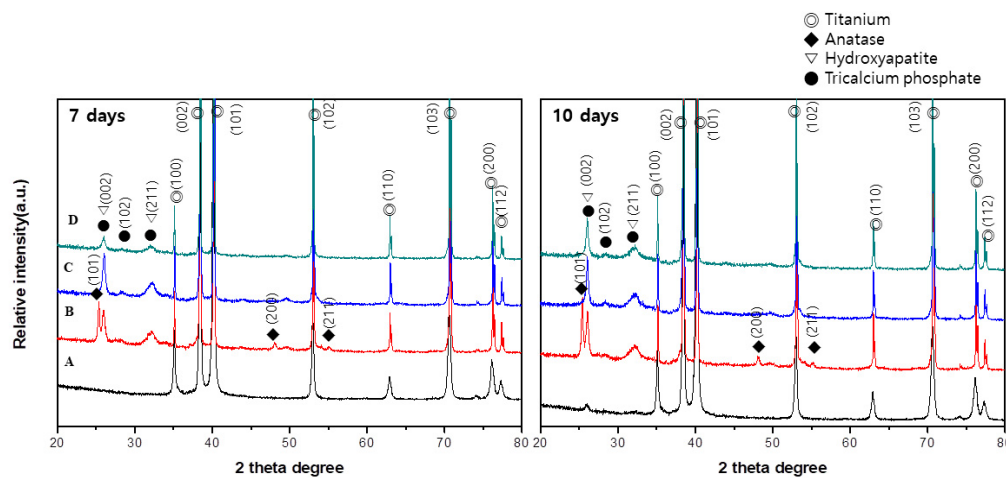
Figure 5. XRD patterns of difference specimens after immersion in SBF for 7 and 10 days: (A) PT; (B) PTN; (C) PTNA; and (D) PTNAC.

Figure 6 shows cell proliferation (Figure 6A) and attachment (Figure 6B) after cell culture for 2 and 5 days. Cell proliferation was not significantly different between all groups after the cells were cultured for 2 days (Figure 6A). Cell proliferation was higher on PT than the other groups after the cells were cultured for 5 days (Figure 6A).

Figure 6B shows the results of the WST assay performed on the specimens treated with 0.02% Trypsin-EDTA for 5 min after cell culture for 2 and 5 days. The cells attachment on the PT and PTNAC was higher than with PTN and PTNA after cell culture for 2 days. The cell adhesion was not significantly different between all groups after cell culture for 5 days. However, compared to the cell proliferation graph, it was confirmed that the cell adhesion rate of the carbon nanotube-coated specimen was improved.
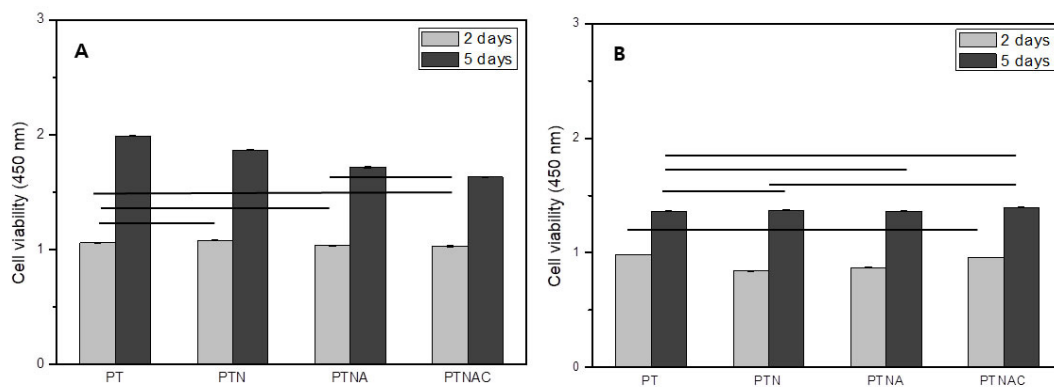
Figure 6. WST assay of (**A**) cell proliferation on the PT, PTN, PTNA, and PTNAC surfaces after cells were cultured for 2 and 5 days; (**B**) adhered cells on the PT, PTN, PTNA, and PTNAC surfaces with 0.02% TryLE™ Express treatment for 5 min.

Figure 7 shows SEM images of cell morphologies after cells were cultured for 2 and 5 days. Cell morphology on PT showed a round shape and high cell density. The cell morphology on PTNA showed an elongated shape for 2 days but a round shape due to developed cytoplasm for 5 days. PTN and PTNAC showed more developed cytoplasm than PTNA.
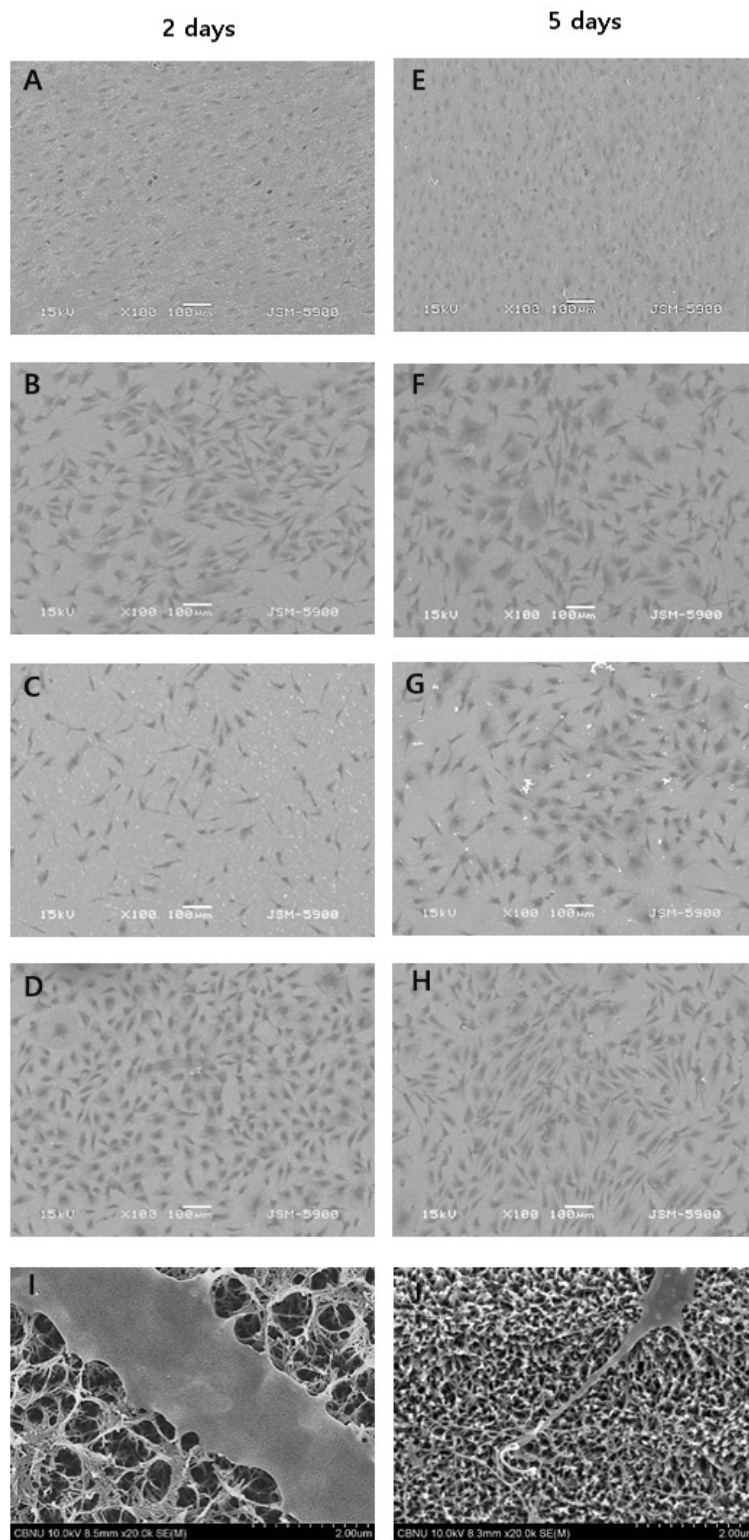
Figure 7. SEM images of cell morphologies: (**A**,**E**) PT, (**B**,**F**) PTN, (**C**,**G**) PTNA, and (**D**,**H**) PTNAC after the (**A**–**D**) 2 and (**E**–**H**) 5 days MC3T3-E1 cell cultures and (**I**) PTNA, and (**J**) PTNAC with a high magnification.
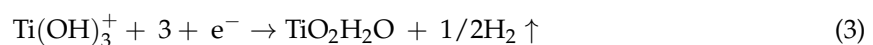
4. Discussion

For successful osseointegration after implant surgery, cell compatibility is important. In other words, the incipient osteoblast adhesion, proliferation, and differentiation are crucial factors. To enhance the efficiency of osseointegration, a variety of surface treatment methods have recently been attempted. In particular, research into increasing the bioactivity of the titanium implant surface for early rapid bone formation have been continuously carried out [21,22]; incipient osteoblast formation is closely related to the implant surface properties. This study investigated the surface bioactivity and biocompatibility by changing the characteristics of the titanium surfaces. To enhance bioactivity of the titanium surface, radially elongated nanoscale hairy structures were formed by soaking the anodized titanium surface in an alkaline solution, followed by MWCNT coating. After that, the coating-dependent surface characteristics, HAp formation ability, and the interactions between osteoblasts and the surface-modified titanium were evaluated to determine its suitability as a biomaterial.

In this study, titanium was anodized in an electrolyte containing NHF_4. The anodized surface confirmed that nano-sized pores were formed in a homogeneous structure (Figure 1B). At this time, the mechanism of the TiO_2 nanotube layer formation by anodic oxidation on the surface of titanium is seen to be the result of the growth of a dense oxide film layer which occurs electrochemically and because of the decomposition of oxide by fluorine ions. When the anodic oxidation process is performed under a condition of constant voltage, since an oxide film layer of a constant thickness is formed on the surface, the intensity of the electric field is radically reduced, so that the current shows an exponential decrease and reaches a state of equilibrium. However, because of the decomposition action of the fluorine ions liberated from the soluble fluorine compound contained in the electrolytic solution, the surface layer is activated again so that a large number of pores are generated, the reduced current slightly increases, and grows into dense nanotubes that form into a regular array [23,24]. The anodized titanium was immersed in a 5M NaOH solution for 24 h and heat-treated to form a dense network on the surface (Figure 1C). The network structure of the alkali treatment was generated as follows. The alkali treatment with sodium hydroxide corrodes the titanium oxide film by the hydroxyl, and the reaction formula is as follows [25]:

$$TiO_2 \; + \; NaOH \rightarrow Ti(OH)_3^+ \; + \; Na^+ \tag{1}$$

This reaction is assumed to occur concurrently with titanium hydration.

$$Ti \; + \; 3OH^- \rightarrow Ti(OH)_3^+ \; + \; 4e^- \tag{2}$$

$$Ti(OH)_3^+ \; + \; 3 + \; e^- \rightarrow TiO_2H_2O \; + \; 1/2H_2 \uparrow \tag{3}$$

$$Ti(OH)_3^+ \; + \; OH^- \leftrightarrow Ti(OH)_4 \tag{4}$$

Negatively charged hydrates are formed on the matrix surface when the hydroxyl group is further added to the hydrated TiO_2.

$$TiO_2 \cdot H_2O \; + \; OH^- \leftrightarrow HTiO_3^- \cdot nH_2O \tag{5}$$

These negatively charged hydrates bind to the alkali ions in the solution to form an alkali titanate hydroxide gel layer, resulting in a structurally heterogeneous porous net structure. The hydroxide gel layer is dehydrated under heat treatment and undergoes densification and forms stable amorphous crystalline sodium titanate, thus modifying the composition and structure of the surface layer. In addition, in this study, carbon nanotubes were coated on the titanium surface after the above surface treatment. The only alkali treated surface on the titanium and TiO_2 formed titanium surface (PTNA) are similar in appearance [26]. However, it was identified that the heat-treated surface after the alkali treatment on the TiO_2 nanotube has a more uniform and dense surface than the surface only

treated with alkali in the previous study [4]. TiO_2 nanotube surfaces provide a favorable template for bone cell growth and differentiation [27]. Also, the porous surface of TiO_2 increases the initial osseointegration [28,29]. Moreover, higher O ion concentration in the TiO_2 layer formed by anodization can make Na^+ react more easily during alkali treatment than the surface of untreated titanium, which results in the formation of amorphous sodium titanate [30]. This amorphous sodium titanate in the TiO_2 layer can enhance initial bone formation more than when only a TiO_2 layer exists on the titanium surface.

CNT is a new material that is attracting attention in various research fields due to its excellent electrical conductivity and excellent physical and chemical properties. In addition, studies for applying CNTs as biomaterials have been increasing. After the carbon nanotube coating, the surface showed a more complicated network structure after the alkali treatment, and the presence of carbon nanotubes on the surface was also confirmed (Figure 1D).

As a result of XRD, peaks of anatase and rutaile phases were found in the PTN group. The PTNA and PTNAC groups also showed weak an anatase phase and Na_2TiO_3 phase (Figure 2). If TiO_2 formed on the titanium surface anodized in an electrolyte solution containing NH_4F and glycerol undergoes heat treatment, the anatase phase begins to form at 500 °C. In general, if a titanium specimen is heat-treated at around 600 °C after 24 h immersion in 5 M NaOH at 60 °C, crystalline a sodium titanate phase appears [4].

Cells are generally adhered onto the rough surface of biomaterials. Factors that play an important role in the cell attachment process are surface roughness, wettability, and surface energy. In this study, the surface roughness of titanium increased through the treatment of the surface when compared with PT (Figure 3). The surface roughness of PTNAC (among the surface-treated titanium in this study) was lowest since the CNTs were coated on the porous structure of TiO_2 by the alkali treatment. The surface with the high roughness generally shows high hydrophilicity. Highly hydrophilic surfaces makes organisms grow well, which is directly related to biocompatibility [31]. The highly hydrophilic surface of titanium results in superior cell adhesion and cell proliferation [31]. In this study, the surface of the titanium had a low contact angle when compared with the surface of PT. The PTNA group showed the lowest contact angle. The PTNAC group showed a higher contact angle than the PTN and PTNA groups since the CNTs coated on the surface decreased hydrophilic characteristics on the surfaces. However, the value of the contact angle for all groups was less than 90 degrees, which means the surfaces of all groups had a hydrophilic surface [32].

The formation of apatite, a bone-like material, is of vital importance for biostability and osseointegration performance. In particular, if the titanium surface is treated with NaOH, a sodium titanate gel layer containing alkaline ions is formed. Such a titanium surface net structure is extremely dense and refines apatite, thus promoting the formation of amorphous sodium titanate [11,33,34]. In this study, the apatite-forming ability was tested by immersing each surface-treated titanium specimen in a SBF solution for 7 and 10 days (Figures 4 and 5); precipitates were confirmed on the surface of PTN, PTNA, and PTNAC after immersion for 7 days (Figure 4). The XRD observations revealed the formation of HAp (Figure 5). After the 10-day immersion, apatite was found to cover the surfaces of all specimens. The ionization of KH_2PO_4 and Na_2HPO_4 components in the SBF solution releases hydrogen ions, forming H_3O^+ ions by binding to water molecules. If an alkali-treated specimen is soaked in a SBF solution, Na^+ on the surface and H_3O^+ in the SBF solution are substituted to form the Ti–OH group, and if left to react further with the SBF solution, it binds with Ca^+ to form calcium titanate. Such a surface induces binding with PO_4^{2-}, thereby forming amorphous calcium phosphate, which then grows in the order of DCP-OCP-TCP-HAp [14,23,35]. As such, the higher the hydrophilicity of the surface, the greater the HAp induction through the enhanced surface–SBF contact.

This study investigated the effect multiple-surface treated titanium had on cell growth. Cell proliferation was confirmed on each treated specimen after MC3T3-E1 cells were cultured for 2 days and 5 days (Figure 6A). In this study, cell proliferation was not significantly different ($p > 0.05$) after cells were cultured for 2 days when the specimens of treated surface (PTN, PTNA, and PTNAC)

were compared to PT. In addition, cell proliferation decreased with added surface treatment after cells were cultured for 5 days. However, improved cell proliferation was confirmed in all groups after 5 days of cell culture. This may be explained by looking at a previous report that states that while the alkali-treated titanium surface shows a high apatite formation efficiency in the SBF solution, the amorphous sodium titanate layer formed on the surface releases sodium ions during implantation, thereby forming narrow-spaced pores and thus negatively affecting cell reactions [16]. The alkaline treated PTNA and PTNAC groups have a favorable surface affinity for bonding with organisms. However, the surface obtained by the alkali treatment reacted with the culture medium and showed low cell proliferation because Na ions were eluted.

In this study, the cells attached to the surface of each group were examined by WST assay after 0.02% TryLE™ Express treatment for 5 min (Figure 6B). After 2 days of cell culture, the attached cells were higher on the PT and PTNAC surfaces. In addition, there was no statistically significant difference in all specimens after cell culture for 5 days. However, compared to the cell proliferation graph, it was confirmed that the cell adhesion rate of the carbon nanotube-coated specimen (PTNAC) was improved. It is considered that the carbon nanotube affects cell adhesion. A previous study reported that CNTs exhibited a strong cell adhesion ability and attributed it to the mechanical bonding between the cell surface or filopodia and the protein adsorbed in CNTs [36]. According to a study conducted by Terada et al. [37], a collagen-coated dish showed higher cell proliferation and viability rates compared with a MWCNT-coated dish, but the latter showed stronger cell adhesion than the former. Aoki et al. [38] and Zanello et al. [39] reported that when osteoblasts were cultured in MWCNTs, the MWCNTs showed the same mechanical contact as the osteoblasts, and explained that this mechanical bonding is one of the reasons for the high bonding strength and that the large specific area of MWCNTs also contributes to the increased adhesion ability.

In order for cells to survive, adsorption of the cells into the surfaces should be stable, followed by proliferation. MT3T3-E1 osteoblasts extend filopodia to the surface for stable adsorption. As a result of observing the adsorption state of cells, including filopodia, during the adsorption process of the MC3T3-E1 osteoblast, more cells were adsorbed on the surface coated with carbon nanotubes (Figure 7). This suggests that the surface coated with carbon nanotubes helps the cells to adsorb more strongly and that the strong adsorption of these cells is the result of the effect of MWCNT.

5. Conclusions

A uniformly arrayed TiO_2 NT layer was formed on the surface of Ti by anodization. A radially elongated nanoscale hairy structure was formed on the TiO_2 NT layer by an alkali treatment, and an MWCNT covered the entire surface with a complex network structure. Surface roughness increased in the order of PT < PTNAC < PTN < PTNA. The contact angle decreased in the other of PT < PTNAC < PTN < PTNA.

Whereas PTNA showed a superior HAp formation ability compared with the other surface-treated groups after immersion in SBF; the PT group and PTNAC group had the highest cell proliferation and cell adhesion ability, respectively.

Author Contributions: J.-E.P., Y.-S.J. and M.-H.L. conceived and designed the experiments; J.-E.P. performed the experiments; Y.-S.J., T.-S.B. and M.-H.L. analyzed the data; J.-E.P., Y.-S.J. and M.-H.L. cooperatively wrote this article.

References

1. Brunette, D.M.; Tengvall, P.; Textor, M.; Thomsen, P. *Titanium in Medicine: Material Science, Surface Science, Engineering, Biological Responses and Medical Applications*; Springer Science & Business Media: Berlin, Germany, 2012.

2. Brammer, K.S.; Choi, C.; Frandsen, C.J.; Oh, S.; Johnston, G.; Jin, S. Comparative cell behavior on carbon-coated TiO_2 nanotube surfaces for osteoblasts vs. osteo-progenitor cells. *Acta Biomater.* **2011**, *7*, 2697–2703. [CrossRef] [PubMed]

3. Terada, M.; Abe, S.; Akasaka, T.; Uo, M.; Kitagawa, Y.; Watari, F. Multiwalled carbon nanotube coating on titanium. *Bio-Med. Mater. Eng.* **2009**, *19*, 45–52.

4. Kim, S.Y.; Kim, Y.K.; Park, I.S.; Jin, G.C.; Bae, T.S.; Lee, M.H. Effect of alkali and heat treatments for bioactivity of TiO_2 nanotubes. *Appl. Surf. Sci.* **2014**, *321*, 412–419. [CrossRef]

5. Kim, H.L.; Park, I.S.; Lee, S.J.; Yu, M.K.; Lee, K.W.; Bae, T.S.; Lee, M.H. Effect of surface pretreatment and pack cementation on bioactivity of titanium dental implant. *Surf. Coat. Technol.* **2014**, *259*, 178–184. [CrossRef]

6. Wen, H.; Liu, Q.; De Wijn, J.; De Groot, K.; Cui, F. Preparation of bioactive microporous titanium surface by a new two-step chemical treatment. *J. Mater. Sci. Mater. Med.* **1998**, *9*, 121–128. [CrossRef] [PubMed]

7. Chen, Y.-F.; Lee, C.-Y.; Yeng, M.-Y.; Chiu, H.-T. Preparing titanium oxide with various morphologies. *Mater. Chem. Phys.* **2003**, *81*, 39–44. [CrossRef]

8. Lim, Y.J.; Oshida, Y.; Andres, C.J.; Barco, M.T. Surface characterizations of variously treated titanium materials. *Int. J. Oral Maxillofac. Implants* **2001**, *16*, 333–342. [PubMed]

9. Das, K.; Bose, S.; Bandyopadhyay, A. TiO_2 nanotubes on Ti: Influence of nanoscale morphology on bone cell–materials interaction. *J. Biomed. Mater. Res. Part A* **2009**, *90*, 225–237. [CrossRef] [PubMed]

10. He, J.; Zhou, W.; Zhou, X.; Zhong, X.; Zhang, X.; Wan, P.; Zhu, B.; Chen, W. The anatase phase of nanotopography titania plays an important role on osteoblast cell morphology and proliferation. *J. Mater. Sci. Mater. Med.* **2008**, *19*, 3465–3472. [CrossRef] [PubMed]

11. Kim, H.; Miyaji, F.; Kokubo, T.; Nakamura, T. Effect of heat treatment on apatite-forming ability of Ti metal induced by alkali treatment. *J. Mater. Sci. Mater. Med.* **1997**, *8*, 341–347. [CrossRef] [PubMed]

12. Kim, H.W.; Kim, H.E.; Salih, V.; Knowles, J.C. Sol-gel-modified titanium with hydroxyapatite thin films and effect on osteoblast-like cell responses. *J. Biomed. Mater. Res. Part A* **2005**, *74*, 294–305. [CrossRef] [PubMed]

13. Kokubo, T.; Kim, H.-M.; Kawashita, M.; Nakamura, T. REVIEW Bioactive metals: Preparation and properties. *J. Mater. Sci. Mater. Med.* **2004**, *15*, 99–107. [CrossRef] [PubMed]

14. Kokubo, T.; Miyaji, F.; Kim, H.M.; Nakamura, T. Spontaneous formation of bonelike apatite layer on chemically treated titanium metals. *J. Am. Ceram. Soc.* **1996**, *79*, 1127–1129. [CrossRef]

15. Nishiguchi, S.; Nakamura, T.; Kobayashi, M.; Kim, H.-M.; Miyaji, F.; Kokubo, T. The effect of heat treatment on bone-bonding ability of alkali-treated titanium. *Biomaterials* **1999**, *20*, 491–500. [CrossRef]

16. Petek Korkusuz, S.S.; Puralı, N.; Görür, İ.; Önder, E.; Nohutçu, R.; Koç, N.; Timucin, M.; Öztürk, A.; Korkusuz, F. Interaction of MC3T3-E1 cells with titanium implants. *Jt. Dis. Relat. Surg.* **2008**, *19*, 84–90.

17. Uchida, M.; Kim, H.M.; Kokubo, T.; Fujibayashi, S.; Nakamura, T. Effect of water treatment on the apatite-forming ability of NaOH-treated titanium metal. *J. Biomed. Mater. Res. Part A* **2002**, *63*, 522–530. [CrossRef] [PubMed]

18. Iijima, S. Helical microtubules of graphitic carbon. *Nature* **1991**, *354*, 56–58. [CrossRef]

19. Liang, F.; Chen, B. A review on biomedical applications of single-walled carbon nanotubes. *Curr. Med. Chem.* **2010**, *17*, 10–24. [CrossRef] [PubMed]

20. Saito, N.; Usui, Y.; Aoki, K.; Narita, N.; Shimizu, M.; Hara, K.; Ogiwara, N.; Nakamura, K.; Ishigaki, N.; Kato, H. Carbon nanotubes: Biomaterial applications. *Chem. Soc. Rev.* **2009**, *38*, 1897–1903. [CrossRef] [PubMed]

21. Jonášová, L.; Müller, F.A.; Helebrant, A.; Strnad, J.; Greil, P. Biomimetic apatite formation on chemically treated titanium. *Biomaterials* **2004**, *25*, 1187–1194. [CrossRef] [PubMed]

22. Kim, H.M.; Miyaji, F.; Kokubo, T.; Nakamura, T. Preparation of bioactive Ti and its alloys via simple chemical surface treatment. *J. Biomed. Mater. Res.* **1996**, *32*, 409–417. [CrossRef]

23. Kaneco, S.; Chen, Y.; Westerhoff, P.; Crittenden, J.C. Fabrication of uniform size titanium oxide nanotubes: Impact of current density and solution conditions. *Scr. Mater.* **2007**, *56*, 373–376. [CrossRef]

24.　Macak, J.M.; Tsuchiya, H.; Ghicov, A.; Yasuda, K.; Hahn, R.; Bauer, S.; Schmuki, P. TiO$_2$ nanotubes: Self-organized electrochemical formation, properties and applications. *Curr. Opin. Solid State Mater. Sci.* **2007**, *11*, 3–18. [CrossRef]

25.　Liu, X.; Chu, P.K.; Ding, C. Surface modification of titanium, titanium alloys, and related materials for biomedical applications. *Mater. Sci. Eng. R Rep.* **2004**, *47*, 49–121. [CrossRef]

26.　Xing, H.; Komasa, S.; Taguchi, Y.; Sekino, T.; Okazaki, J. Osteogenic activity of titanium surfaces with nanonetwork structures. *Int. J. Nanomed.* **2014**, *9*, 1741–1755. [CrossRef] [PubMed]

27.　Popat, K.C.; Leoni, L.; Grimes, C.A.; Desai, T.A. Influence of engineered titania nanotubular surfaces on bone cells. *Biomaterials* **2007**, *28*, 3188–3197. [CrossRef] [PubMed]

28.　Bandyopadhyay, A.; Shivaram, A.; Tarafder, S.; Sahasrabudhe, H.; Banerjee, D.; Bose, S. In vivo response of laser processed porous titanium implants for load-bearing implants. *Ann. Biomed. Eng.* **2017**, *45*, 249–260. [CrossRef] [PubMed]

29.　Bjursten, L.M.; Rasmusson, L.; Oh, S.; Smith, G.C.; Brammer, K.S.; Jin, S. Titanium dioxide nanotubes enhance bone bonding in vivo. *J. Biomed. Mater. Res. Part A* **2010**, *92*, 1218–1224.

30.　Oh, S.-H.; Finones, R.R.; Daraio, C.; Chen, L.-H.; Jin, S. Growth of nano-scale hydroxyapatite using chemically treated titanium oxide nanotubes. *Biomaterials* **2005**, *26*, 4938–4943. [CrossRef] [PubMed]

31.　Das, K.; Bose, S.; Bandyopadhyay, A. Surface modifications and cell–materials interactions with anodized Ti. *Acta Biomater.* **2007**, *3*, 573–585. [CrossRef] [PubMed]

32.　Prodana, M.; Duta, M.; Ionita, D.; Bojin, D.; Stan, M.S.; Dinischiotu, A.; Demetrescu, I. A new complex ceramic coating with carbon nanotubes, hydroxyapatite and TiO$_2$ nanotubes on Ti surface for biomedical applications. *Ceram. Int.* **2015**, *41*, 6318–6325. [CrossRef]

33.　Kim, H.M.; Miyaji, F.; Kokubo, T.; Nakamura, T. Apatite-forming ability of alkali-treated Ti metal in body environment. *J. Ceram. Soc. Jpn.* **1997**, *105*, 111–116. [CrossRef]

34.　Kim, H.M.; Miyaji, F.; Kokubo, T.; Nakamura, T. Bonding strength of bonelike apatite layer to Ti metal substrate. *J. Biomed. Mater. Res. Part A* **1997**, *38*, 121–127. [CrossRef]

35.　Kim, H.-M.; Takadama, H.; Kokubo, T.; Nishiguchi, S.; Nakamura, T. Formation of a bioactive graded surface structure on Ti–15Mo–5Zr–3Al alloy by chemical treatment. *Biomaterials* **2000**, *21*, 353–358. [CrossRef]

36.　Li, X.; Chen, W.; Zhan, Q.; Dai, L.; Sowards, L.; Pender, M.; Naik, R.R. Direct measurements of interactions between polypeptides and carbon nanotubes. *J. Phys. Chem. B* **2006**, *110*, 12621–12625. [CrossRef] [PubMed]

37.　Terada, M.; Abe, S.; Akasaka, T.; Uo, M.; Kitagawa, Y.; Watari, F. Development of a multiwalled carbon nanotube coated collagen dish. *Dent. Mater. J.* **2009**, *28*, 82–88. [CrossRef] [PubMed]

38.　Aoki, N.; Yokoyama, A.; Nodasaka, Y.; Akasaka, T.; Uo, M.; Sato, Y.; Tohji, K.; Watari, F. Cell culture on a carbon nanotube scaffold. *J. Biomed. Nanotechnol.* **2005**, *1*, 402–405. [CrossRef]

39.　Zanello, L.P.; Zhao, B.; Hu, H.; Haddon, R.C. Bone cell proliferation on carbon nanotubes. *Nano Lett.* **2006**, *6*, 562–567. [CrossRef] [PubMed]